

# Optimization and characterization of a femtosecond tunable light source based on the soliton self-frequency shift in photonic crystal fiber

C. H. Hage <sup>a</sup>, B. Kibler <sup>a</sup>, E.R. Andresen <sup>b</sup>, S. Michel <sup>b</sup>, H. Rigneault <sup>b</sup>, A. Courjaud <sup>c</sup>, E. Mottay <sup>c</sup>,  
J.M. Dudley <sup>d</sup>, G. Millot <sup>a</sup> and C. Finot <sup>\*a</sup>

<sup>a</sup> Laboratoire Interdisciplinaire Carnot de Bourgogne, UMR 5209 CNRS-UB, Dijon, France;

<sup>b</sup> Institut Fresnel, UMR 6133, Marseille, France

<sup>c</sup> Amplitude Systèmes, Pessac, France

<sup>d</sup> Institut Femto-ST, UMR 6174, Besançon, France

## ABSTRACT

We take advantage of the Raman soliton self-frequency shift experienced during the propagation in an anomalous dispersive photonic crystal fiber in order to continuously tune the central frequency of ultrashort pulses. We discuss the fiber properties to be favored to obtain high power spectral densities and we carry out an extensive experimental study of the properties of the frequency shifted pulses in terms of spectral, autocorrelation, and RF spectrum measurements.

**Keywords:** temporal solitons and pulse propagation, Raman scattering, photonic crystal fiber.

## 1. INTRODUCTION

Nonlinear optics in fibers provides a very wide panel of attractive solutions in order to generate new optical spectral components: self-phase modulation, four wave mixing, Raman Stokes generation or intrapulse Raman scattering <sup>1</sup>. This latest phenomenon leads to a progressive shift towards lower frequencies of the central frequency of ultrashort pulses propagating in an anomalous dispersive fiber. Therefore this effect known as the Raman soliton self-frequency shift (SSFS) <sup>2</sup> is an efficient way to continuously tune the wavelength of a femtosecond source. Typical shifts over several hundreds of nanometers have been already reported. The first demonstrations have been carried out in the telecommunication window around 1550 nm <sup>2,3</sup>. But progresses in the design and fabrication of microstructured fibers have also opened the way for anomalous dispersion below 1.3  $\mu\text{m}$  <sup>4</sup> so that it has become possible to benefit from this technique at the typical wavelengths of ytterbium-doped fiber oscillators and titanium-sapphire lasers <sup>5</sup>. An additional advantage of the microstructure is to enable a reduced mode field diameter so that the nonlinear process under action becomes highly power efficient.

We report here an extensive experimental study dealing with the optimization and the full characterization of a photonic crystal fiber (PCF)-based light source for generating femtosecond tunable pulses that are suitable for coherent anti-Stokes Raman scattering (CARS) microscopy <sup>6</sup>. We first describe our experimental setup and a simple qualitative analysis that enables us to optimize our choice of fiber. We then compare the experimental results obtained with three PCFs and discuss the effects that limit our spectral shift. Finally, a study of the temporal properties is carried out, as well as measurements of the temporal and amplitude jitters of the frequency shifted pulse train.

\* [christophe.finot@u-bourgogne.fr](mailto:christophe.finot@u-bourgogne.fr); phone +33 (0)3 80 39 59 26; fax +33 (0)3 80 39 59 71

## 2. EXPERIMENTAL SETUP AND PRELIMINARY ANALYSIS

The experimental setup we have implemented is sketched in figure 1. We consider the nonlinear evolution of an ultrashort pulse (FWHM of 190 fs, central wavelength 1033 nm) having a Gaussian temporal profile. This pulse is transform-limited and is delivered by a diode pumped passively modelocked laser (Amplitude Systemes, t-Pulse) with a repetition rate of 48 MHz and an average power up to 1 W (corresponding to a maximum pulse energy of 20 nJ per pulse).

The ultrashort pulses are injected in a microstructured fiber having the anomalous dispersion required for the existence of optical solitons<sup>1</sup>. Three different fibers commercialized by the NKT Photonics society are compared: the NL-1.7-785 fiber (**fiber A**), the NL-1.7-765 fiber (**fiber B**) and the NL-1.8-710 fiber (**fiber C**) having zero dispersion wavelengths at respectively 785, 765 and 710 nm and core diameters of 1.7 and 1.8  $\mu\text{m}$ <sup>7</sup>.

Light is coupled into the fiber thanks to a microlens (a typical launching efficiency around 30 % is achieved). A nanotrack device with an active feedback is used so as to optimize the long term stability of the device and to avoid thermal and mechanical drifts<sup>8</sup> (see subsection 3.3). Polarization plates are used to adjust the power launched into the PCF. The half-wave plate is mounted on a motorized rotation device and is controlled via a LabView interface in order to finely tune the power. The polarizer ensures that the light is launched along a neutral axis of the PCF. Let us note that the association of polarization plates can be advantageously replaced by an acousto-optic or an electro-optic device which benefits from a much better response-time than a mechanical rotation mount<sup>9</sup>.

At the output of the PCF, the frequency shift of the pulse is evaluated thanks to an optical spectrum analyzer (Anritsu MS9710B). A long-pass spectral filter is also inserted to remove the non-shifted residue of the pump and the filtered signal is monitored through power measurement, autocorrelation signal (Femtochrome autocorrelator) and RF spectrum signal. The results of those measurements are described in sub-sections 3.1, 3.2 and 3.3, respectively.

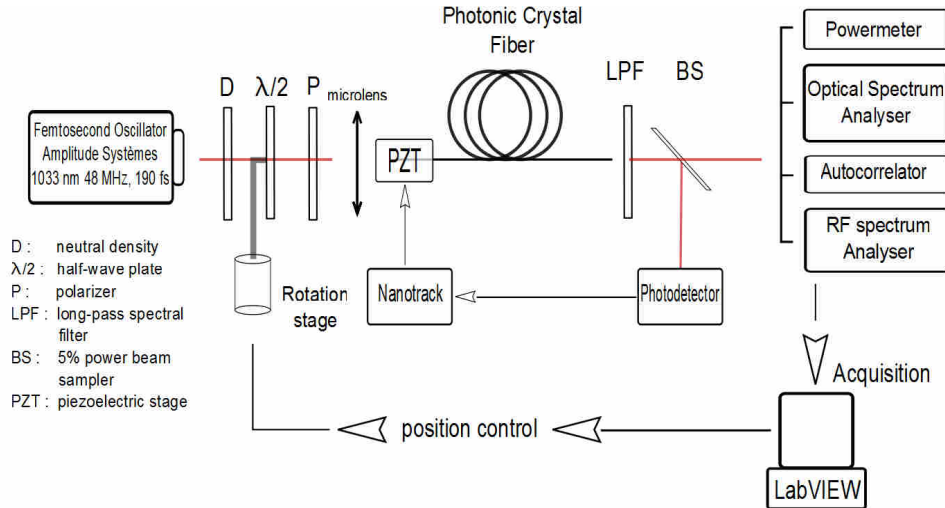


Figure 1. Experimental setup.

A crucial point to keep in mind in order to optimize the system is that the frequency shifted pulses are fundamental solitons<sup>2, 10, 11</sup>. This imposes a stringent relationship between the parameters of the second-order dispersion  $\beta_2$ , the Kerr nonlinearity of the fiber, the peak-power of the pulse and its typical temporal duration<sup>1</sup>. It can then easily be shown that the energy spectral density  $D$  is directly proportional to the ratio  $\beta_2 / \gamma$ .

Therefore, in order to increase  $D$  and to achieve typical values above one pJ/nm which are required to CARS experiments<sup>6</sup>, we will favor a microstructured fiber with a high second order dispersion at the pumping wavelength combined with a reduced nonlinearity. Such a choice is also beneficial to avoid the unwanted transfer of energy towards

lower wavelengths through the generation of dispersive waves<sup>10</sup>. Our choice differs from the PCF parameters that are usually involved in the generation of octave spanning supercontinua where the pumping wavelength is chosen in the vicinity of the zero dispersion wavelength (ZDW) and where high nonlinearity is favored in order to reduce the required input power.

Note that having high second order anomalous dispersion and reduced nonlinearity may be hard to achieved simultaneously around 1030 nm with standard PCF designs as a ZDW located at short wavelengths usually requires a very small fiber core diameter (typically below 2  $\mu\text{m}$  of diameter), thus leading to a strong field confinement and high nonlinearity. Alternate promising solutions already exist such as hollow core fibers<sup>12</sup> or solid core photonic bandgap fibers<sup>13, 14</sup>.

### 3. EXPERIMENTAL RESULTS

#### 3.1 Frequency shifting of the pulses and limiting effects

The spectral evolution is plotted on figure 2 as a function of the initial pulse energy for each fiber used. Automated recording of the optical spectra enables a detailed study of the nonlinear dynamics of the frequency shifted solitons.

Fiber A (figure 2a) is the fiber having the lowest dispersion value at the pumping wavelength. The resulting soliton experiences SSFS for low input powers. However, the frequency shift is stopped around 1250 nm when the pulse approaches the second zero dispersion wavelength of this fiber which has a concave dispersion profile. A dispersive wave is generated around 1350 nm<sup>15</sup>, which could be helpful to determine experimentally the position of the second ZDW<sup>16</sup>. Remark that for this fiber multiple solitons resulting from the initial pulse splitting are generated for initial energies as low as 90 pJ. We also note that the second ejected soliton may interact with the dispersive wave<sup>11, 17</sup> leading to the spectral broadening observed around 1450 nm.

Tests carried out with fiber B which exhibits a higher dispersion outlines that a single soliton can be frequency shifted for energies as high as 160 pJ (figure 2b). The second ZDW being located at higher wavelengths, the pulse can be frequency shifted up to 1350 nm.

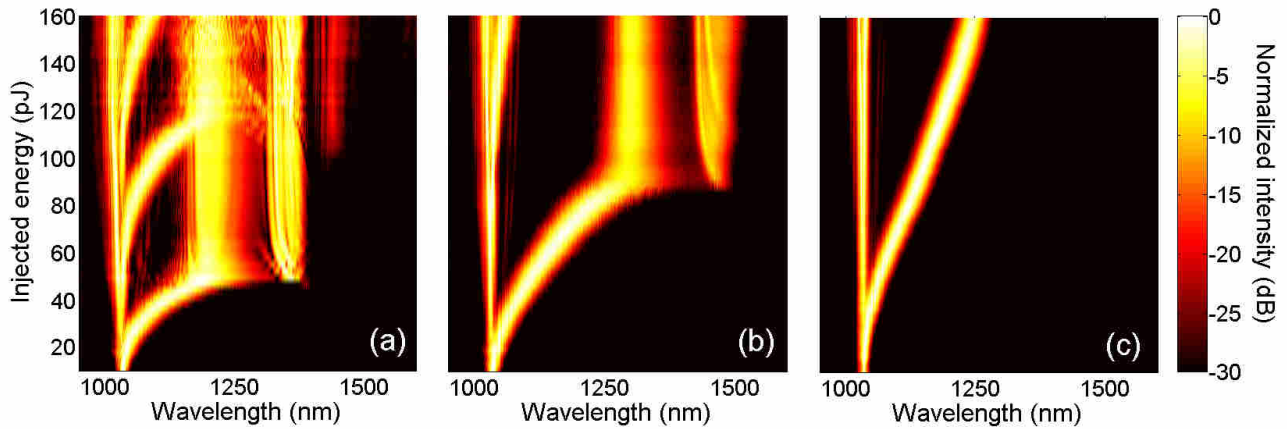


Figure 2. Experimental evolution of the spectral intensity profiles according to the input energy for three different fibers: fiber A, fiber B and fiber C (subplots a, b and c respectively).

Fiber C (figure 2c) is the fiber with the highest dispersion, which favors a frequency shifted soliton with higher energy. The possibility to efficiently tune the central wavelength of a single pulse over a wide range is illustrated on figure 3b. A more quantitative study of the energy that can be frequency shifted is presented in figure 3a and emphasizes the benefits of this fiber compared to the first two ones. Indeed, for fibers A and B, the energy that can be ‘stored’ in a single soliton is limited to 40 and 60 pJ, respectively, the energy leading to a frequency shift up to the second ZDW acting as an upper limit. Fiber C does not have such a second ZDW, which enables to shift the soliton up to 1380 nm (i.e.  $2500\text{ cm}^{-1}$ ), which can be already enough to get access to several vibrational frequencies of biological interest. From figure 2, we can also

see that the spectral width of the frequency shifted pulses is much lower for fiber C, which is favorable to a high energy density.

Note that for fiber C, the physical process that limits the Raman SSFS is the fiber losses that are linked to the absorption of hydroxyl groups around 1380 nm. Therefore increasing the initial energy above 250 pJ will not help to further enhance the energy contained in the shifted soliton. Besides the losses (as well as in a much lesser extend the continuous increase of the dispersion<sup>18</sup>) also manifest themselves in the progressive decrease of the spectral width of the soliton (figure 3c).

All in all, we have demonstrated a spectral energy density of 8 pJ/nm for fiber C, whereas fibers A and B are restricted to values of 1.5 pJ/nm and 2.5 pJ/nm respectively.

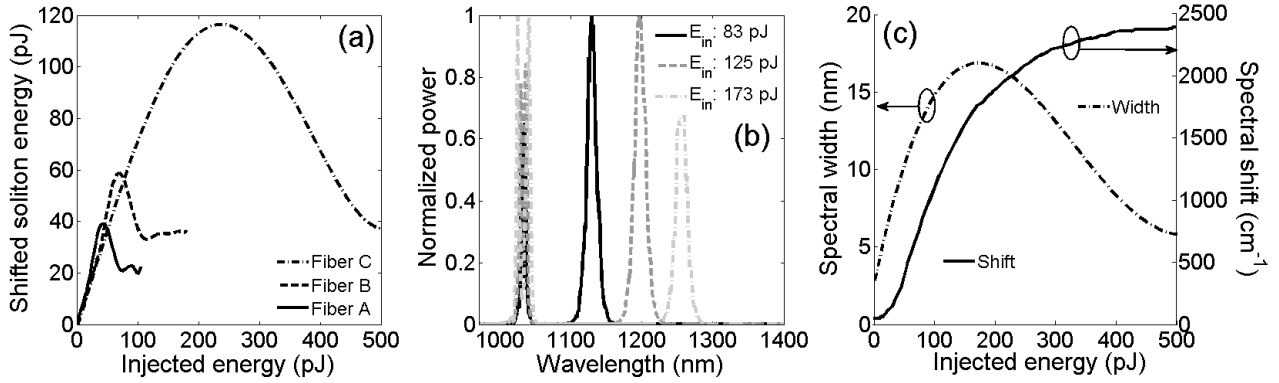


Figure.3. (a) Evolution of the energy of the frequency shifted soliton according to the input energy for the three fibers under test (PCF A, PCF B and PCF C: solid black line, dashed line and mixed line respectively). Results obtained using fiber C: (b) normalized spectral profiles for three initial energies and (c) evolution of the spectral width (mixed line) and the spectral shift (solid line) according to the input energy. Results obtained for fiber C.

### 3.2 Temporal characterization of the output pulse

The spectral characterization of the frequency shifted pulses in fiber C has been complemented by temporal measurements relying on intensity autocorrelation. The results are shown in figure 4. Subplot (a) outlines the high quality of the output pulses obtained after spectral filtering (to remove unwanted pump residue): no substructure or sidelobes are noticed and the temporal profile is typical of the hyperbolic secant pulse. From figure 4, we can also notice that the frequency shifted pulses are slightly shorter than the initial pulses delivered by the laser.

Evolution of the temporal duration and time-bandwidth product of the output pulses according to the output wavelength is summarized in figure 4b. These results confirm that for a wide range of frequency shifts (output wavelength between 1100 and 1350 nm), a nearly transform-limited hyperbolic secant pulse is obtained (time bandwidth product typically between 0.32 and 0.38). Therefore, the strong spectral narrowing observed when the pulse reaches the spectral window of OH loss directly leads to a significant temporal broadening.

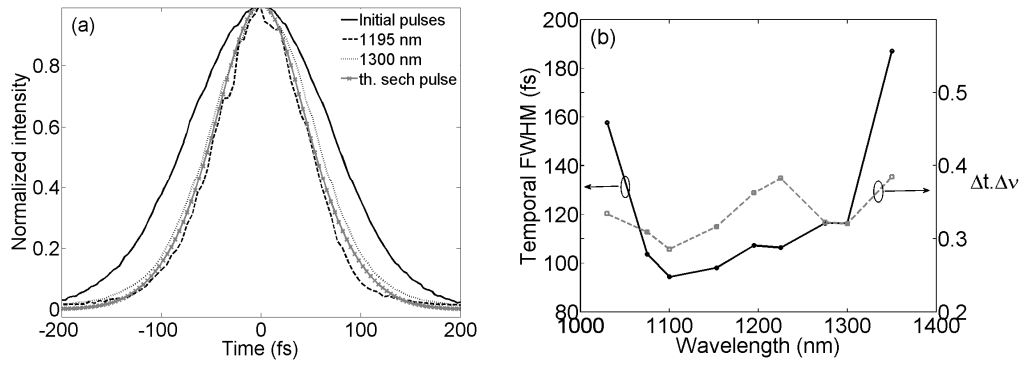


Figure 4. (a) Autocorrelation measurements of the spectrally shifted pulses for three frequency shifts. The temporal profiles obtained after the PCF output are compared to the initial pulse delivered by the laser (solid black line). (b) Evolution of the temporal FWHM (solid black line, hyperbolic secant shape assumed) and of the time-bandwidth product (grey dashed line) according to the wavelength of the output soliton pulse.

### 3.3 Jitters and long term stability of the source

Jitter measurements were finally carried out to check the system stability on two time-scales. The short-time scale allows for measuring the laser and shifted solitons jitters and the long-time scale allows for measuring the possible mechanical or thermal drifts.

The short-term stability study is carried out by using the radio-frequency method<sup>19</sup>, where the optical signal is sent onto a suitable photodetector (5 GHz bandwidth photodiode) which signal is analyzed by an electrical spectrum analyzer (26.5 GHz bandwidth Agilent EXA07). This setup analyses the power spectrum of the periodic signal. Different kinds of jitters can be estimated from the integration of the wings of these peaks, especially amplitude and timing jitters (laser period jitter). Although this method is now a wide-spread method because of its relative simplicity, it may suffer from some drawbacks including precision and lack of thoroughness in determining the different noise sources.<sup>20, 21</sup>

Various harmonics spectra (1st, 10th, 20th, 30th, 40th and 50th harmonics) are recorded for different spectral shifts (an example of those electrical spectra is provided on figure 5a). Results of amplitude and timing jitters are summarized in figure 5b and 5c respectively. Almost constant jitters of 0.15% in relative amplitude and ~300 fs in time are estimated for two resolution bandwidths (RBW - 300 and 30 Hz) and are consistent with previous results demonstrated at telecommunication wavelengths<sup>3</sup>. Our experimental values have been found very similar to the jitters of the initial oscillator itself, so that we can conclude that, with our choice of fiber parameters (fiber C), the nonlinear process involved in the SSFS does not degrade the pulse to pulse stability of our device. Note that having used a configuration where a single pulse is frequency shifted is beneficial to prevent soliton-to-soliton interactions and subsequent degradations leading potentially to so-called rogue events.

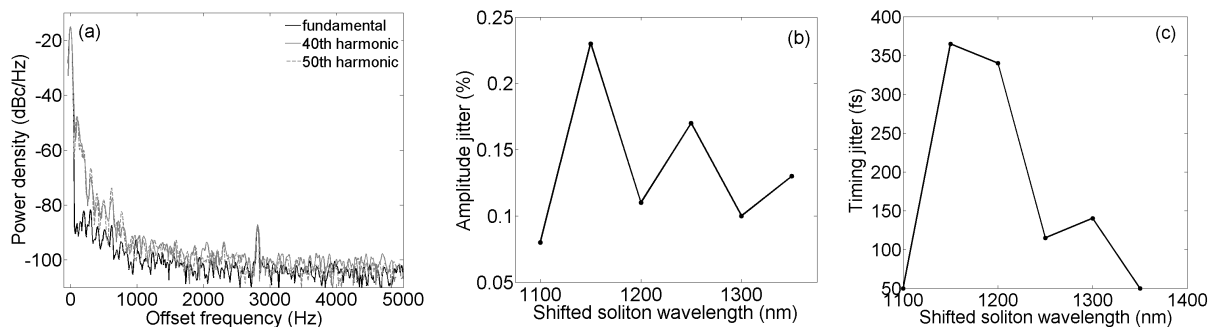


Figure 5. (a) Radio-Frequency spectra, obtained for a RBW of 30 Hz. Spectral power relative to the carrier frequency (dBc/Hz) vs. carrier offset frequency. (b) Amplitude jitter of the frequency shifted soliton as a function of the wavelength. (c) Timing jitter of the frequency shifted soliton as a function of the wavelength.

The long-term study is carried out as the fiber injection can suffer from mechanical drift of the launching device<sup>8</sup>. A several tens of minutes long power monitoring is performed with and without a Thorlabs' Nanotrack system (an actuated piezoelectric flexure stage). The results are shown on figure 6 and outline the clear improvement brought by the Nanotrack system that prevents a continuous power decrease observed when no feedback is provided.

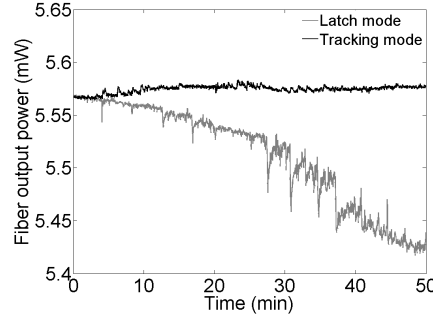


Figure 6. Output power monitoring over a timespan of 50 min. Results obtained in latch and tracking mode are compared (grey and black line respectively).

#### 4. CONCLUSION

We have reported an extensive experimental study dealing with the optimization and the full characterization of a photonic crystal fiber (PCF)-based light source for generating femtosecond tunable pulses that are suitable for coherent anti-Stokes Raman scattering (CARS) microscopy. Starting from a commercial femtosecond oscillator operating at 1033 nm and which delivers 20 nJ/ 190 fs Gaussian transformed-limited pulses, we have taken advantage of the soliton-self frequency shift (SSFS) that induces through Raman scattering a continuous shift of the central wavelength of any ultrashort pulse propagating in a silica fiber.

As a first optimization step, we have experimentally tested the performance of three commercially available PCFs exhibiting distinct group velocity dispersion (GVD) characteristics. The spectral profile of GVD has been found to highly impact the range of tunability of the SSFS process, the presence of a second zero dispersion wavelength being a physical limit. Consequently, a single zero dispersion wavelength has been favored in our setup. Value of the anomalous dispersion also affects the Power Spectral Density (PSD): as frequency shifted pulses are fundamental solitons, the PSD is directly proportional to the ratio of the GVD over the nonlinearity. Using high dispersion value at the pump wavelength, we have achieved a 300  $\mu\text{W}/\text{nm}$  PSD, which is well above the requirement for CARS microscopy (around 50  $\mu\text{W}/\text{nm}$ ). Note that a high dispersion fiber also limits the generation of additional solitonic structures as well as the energy transferred in blue shifted dispersive waves so that a good conversion efficiency from the pump to the frequency shifted signal can be obtained (around 30% in our case).

Regarding the spectral shift that we have achieved, a maximum frequency shift of 340 nm has been obtained which enables to probe up to 2400  $\text{cm}^{-1}$ . The tunability is achieved by simply adjusting the power launched in the PCF and a close to linear dependence of the frequency shift versus the initial power has been recorded. The tunability range has experimentally been limited by the OH absorption of the fiber, constraint that should be easily removed with newly designed low-OH PCFs. Autocorrelation measurements have confirmed that the frequency shifted pulses are nearly transform limited with an output pulse duration of 100 fs.

Additional measurements based on radio-frequency (RF) spectrum analysis were finally carried out in order to estimate the level of amplitude and timing jitters of the output pulses. 0.15% intensity noise and 300-fs timing jitter for any wavelength shifts of the femtosecond soliton pulse have been demonstrated, those values being quite similar to the jitters of the initial oscillator. The long-term stability of the system has been found to be limited by the mechanical drift of the injection device, which can be overcome by using a feedback loop. All the various measurements done have been found to be highly reproducible, which confirms that this wavelength tunable soliton source is stable. Combined with a stage of spectral compression (that can eventually be enhanced by adequate parabolic shaping<sup>22</sup>), this source should be fully suitable for future applications in the context of CARS microscopy<sup>6</sup>.

## ACKNOWLEDGMENT

We thank the French Agence Nationale de la Recherche projects SOFICARS (ANR-07-RIB-013-03) as well as the Conseil Regional de Bourgogne for the grant "Jeunes Chercheurs Entrepreneurs" of Charles Henri Hage.

## REFERENCES

- [1] Agrawal, G. P., [Nonlinear Fiber Optics, Fourth Edition] Academic Press, San Francisco, CA(2006).
- [2] Mitschke, F. M., and Mollenauer, L. F., "Discovery of the soliton self-frequency shift," *Opt. Lett.*, 11(10), 659-661 (1986).
- [3] Matsuo, Y., Nishizawa, N., Mori, M., and Goto, T., "Measurement of timing-jitter in wavelength tunable femtosecond soliton pulses," *Optical Review*, 7(4), 317-322 (2000).
- [4] Russell, P. S. J., "Photonic-Crystal Fibers," *J. Lightw. Technol.*, 24(12), 4729-4749 (2006).
- [5] Cormack, I. G., Reid, D. T., Wadsworth, W. J., Knight, J. C., and Russell, P. S., "Observation of soliton self-frequency shift in photonic crystal fibre," *Electron. Lett.*, 38(4), 167-168 (2002).
- [6] Andresen, E. R., Nielsen, C. K., Thogersen, J., and Keiding, S. R., "Fiber laser-based light source for coherent anti-Stokes Raman scattering microspectroscopy," *Opt. Express*, 15(8), 4848-4856 (2007).
- [7] "NKT Photonics (previously Crystal Fibre)," <http://www.nktphotonics.com>
- [8] Michel, S., Courjaud, A., Mottay, E., Finot, C., Dudley, J. M., and Rigneault, H., "Polarized multiplex CARS using a picosecond laser and a fiber supercontinuum," *Journal of Biomedical Optics*, 16, 021108 (2011).
- [9] Sumimura, K., Ohta, T., and Nishizawa, N., "Quasi-super continuum generation using ultrahigh-speed wavelength-tunable soliton pulses," *Opt. Lett.*, 33(24), 2892-2894 (2008).
- [10] Dudley, J. M., Genty, G., and Coen, S., "Supercontinuum generation in photonic crystal fiber," *Rev. Modern Physics*, 78, 1135-1184 (2006).
- [11] Skryabin, D. V., and Gorbach, A. V., "Looking at a soliton through the prism of optical supercontinuum," *Rev. Modern Physics*, 82, 1287-1299 (2010).
- [12] Gérôme, F., Dupriez, P., Clowes, J., Knight, J. C., and Wadsworth, W. J., "High power tunable femtosecond soliton source using hollow-core photonic bandgap fiber, and its use for frequency doubling," *Opt. Express*, 16(4), 2381-2386 (2008).
- [13] Bétourné, A., Kudlinski, A., Bouwmans, G., Vanvincq, O., Mussot, A., and Quinquempois, Y., "Control of supercontinuum generation and soliton self-frequency shift in solid core photonic bandgap fibres," *Opt. Lett.*, (2009).
- [14] Kibler, B., Martynkien, T., Szpulak, M., Finot, C., Fatome, J., Wojcik, J., Urbanczyk, W., and Wabnitz, S., "Nonlinear femtosecond pulse propagation in an all-solid photonic bandgap fiber," *Opt. Express*, 17(12), 10393-10398 (2009).
- [15] Skryabin, D. V., Luan, F., Knight, J. C., and Russell, J. S., "Soliton self-frequency shift cancellation in photonic crystal fibers," *Science*, 201, 1705-1708 (2003).
- [16] Kibler, B., Finot, C., Gadret, G., Millot, G., Wojcik, J., Szpulak, M., and Urbanczyk, W., "Second zero dispersion wavelength measurement through soliton self-frequency shift compensation in suspended core fibre," *Electron. Lett.*, 44, 1370-1371 (2008).
- [17] Efimov, A., Yulin, A. V., Skryabin, D. V., Knight, J. C., Joly, N., Omenetto, F. G., Taylor, A. J., and Russell, P., "Interaction of an optical soliton with a dispersive wave," *Phys. Rev. Lett.*, 95(21), (2005).
- [18] Fedotov, A. B., Voronin, A. A., Fedotov, I. V., Ivanov, A. A., and Zheltikov, A. M., "Spectral compression of frequency-shifting solitons in a photonic-crystal fiber," *Opt. Lett.*, 34(5), 662-664 (2009).
- [19] Von der Linde, D., "Characterization of the noise in continuously operating mode-locked lasers," *Appl. Phys. B*, 39(4), 201-217 (1986).
- [20] Fuss, I. G., "An interpretation of the spectral measurement of optical pulse train noise," *IEEE J. Quantum Electron.*, 30(11), 2707-2710 (1994).
- [21] Gross, M. C., Hanna, M., Patel, K. M., and Ralph, S. E., "Spectral method for the simultaneous determination of uncorrelated and correlated amplitude and timing jitter," *Appl. Phys. Lett.*, 80(20), 3694-3696 (2002).
- [22] Andresen, E. R., Dudley, J. M., Finot, C., Oron, D., and Rigneault, H., "Transform-limited spectral compression by self-phase modulation of amplitude shaped pulses with negative chirp," *Opt. Lett.*, 36(5), 707-709 (2011).